Phase transition of charged Black Holes in Brans-Dicke theory through geometrical thermodynamics

S. H. Hendi[1,2*], S. Panahiyan[1,3†], B. Eslam Panah[1‡] and Z. Armanfard[1§]
[1] *Physics Department and Biruni Observatory, College of Sciences, Shiraz University, Shiraz 71454, Iran*
[2] *Research Institute for Astronomy and Astrophysics of Maragha (RIAAM), Maragha, Iran*
[3] *Physics Department, Shahid Beheshti University, Tehran 19839, Iran*

In this paper, we take into account black hole solutions of Brans-Dicke-Maxwell theory and investigate their stability and phase transition points. We apply the concept of geometry in thermodynamics to obtain phase transition points and compare its results with those, calculated in canonical ensemble through heat capacity. We show that these black holes enjoy second order phase transitions. We also show that there is a lower bound for the horizon radius of physical charged black holes in Brans-Dicke theory which is originated from restrictions of positivity of temperature. In addition, we find that employing specific thermodynamical metric in the context of geometrical thermodynamics, yields divergencies for thermodynamical Ricci scalar in places of the phase transitions. It will be pointed out that due to characteristics behavior of thermodynamical Ricci scalar around its divergence points, one is able to distinguish the physical limitation point from the phase transitions. In addition, the free energy of these black holes will be obtained and its behavior will be investigated. It will be shown that the behavior of the free energy in the place where the heat capacity diverges, demonstrates second order phase transition characteristics.

arXiv:1511.00598v2 [gr-qc] 28 Jul 2016

I. INTRODUCTION

Einstein's general relativity is able to describe the dynamics of our solar system well enough. In addition, this theory predicted the existence of gravitational waves that recently, was observed by LIGO and Virgo collaboration [1]. It is notable that, observations of the LIGO collaboration could be employed to test the validation of Einstein theory of the gravity or the necessity of modified theories of gravity [2]. Einstein theory of gravity may have some problems in describing gravity accurately at all scales. One of the problems that general relativity faced was that, it couldn't describe the accelerated expansion of the universe accurately [3]. Also, it is consistent with neither Mach's principle nor Dirac's large number hypothesis [4]. Herein, cosmologists explored various alternatives for gravitational fields [5, 6]. The pioneers of studying on scalar-tensor theory were done by Brans and Dicke [7]. This theory accommodates both Mach's principle and Dirac's large number hypothesis [4]. Scientists have investigated various aspects of black holes and gravitational collapse in Brans-Dicke (BD) theory due to their importance in both classical and quantum aspects of gravity [8]. It has been shown that the stationary and vacuum BD solution in $4-$dimensions is just the Kerr solution with a trivial scalar field everywhere [9]. Cai and Myung showed that in $4-$dimensions the BD-Maxwell (BDM) solution is just the Reissner-Nordström (RN) solution with a constant scalar field [10]. However in higher dimensions, due to the fact that the action of Maxwell field is not invariant under conformal transformation and the stress energy tensor of Maxwell field is not traceless, the solution of BDM is RN solution with a nontrivial scalar field.

On the other hand, the black hole thermodynamics has been the field of interest for many researchers since the work of Hawking [11]. Recently, in most treatments of black hole thermodynamics, physicists have considered the cosmological constant (Λ) as a dynamical variable [12, 13]. Furthermore, some authors suggested to treat Λ as a thermodynamic variable [14], such as thermodynamical pressure [15–18]. One of the interesting aspects of the black hole thermodynamics is their stability. In order to have a black hole in thermal stability, its heat capacity must be positive. In other words, positivity of the heat capacity guarantees thermal stability of the black holes. This approach of studying the stability is in the context of the canonical ensemble. Studying the heat capacity of a system also provides a mechanism to study the phase transitions of that system. There are two distinctive points: in one point, changing in the sign of the heat capacity is denoted as a physical limitation point and therefore, the root of the heat capacity is a border between non-physical and physical black hole solutions. Other characterized points are related to divergencies of the heat capacity. We identify these points as second order phase transitions [19].

In the past few decades, applying the thermodynamical geometry for studying the phase transition of black holes has gained lots of attentions. These studies were pioneered by Weinhold [20] and Ruppeiner [21]. Weinhold introduced

* email address: hendi@shirazu.ac.ir
† email address: sh.panahiyan@gmail.com
‡ email address: behzad.eslampanah@gmail.com
§ email address: zahra.armanfard@gmail.com

a metric on the space of equilibrium state and defined the metric tensor as the second derivatives of internal energy with respect to entropy and other extensive quantities. On the other hand, the metric that Ruppeiner introduced was defined as the minus second derivatives of entropy with respect to internal energy and other extensive quantities, which was conformal to Weinhold's metric [22]. However, applying these treatments to study black hole thermodynamics caused some puzzling anomalies. Neither Weinhold nor Ruppeiner metrics were invariant under Legendre transformation. A few years ago, Quevedo [23] proposed an approach to obtain a metric which was Legendre invariant in the space of equilibrium state. His work was based on the observation in which standard thermodynamics was invariant with respect to Legendre transformation. The formalism of geometrothermodynamics (GTD) indicates that phase transition occurs at points where the thermodynamics curvature is singular, as a consequence, the curvature can be interpreted as a measure of thermodynamics interaction. After Quevedo, interesting studies were followed by some authors [24]. Recently, it was pointed out that using the mentioned approaches toward GTD may sometimes confront with some problems. In order to overcome these problems, a new approach was introduced in Ref. [25].

The outline of the paper will be as follow; in Sec. II, we review the charged BD black holes and their thermodynamical quantities. In Sec. III, we introduce the approaches for studying phase transitions of these black holes in the context of heat capacity and geometrical thermodynamics. Then, we investigate the existence of the phase transitions in the context of two mentioned approaches and compare them with each other. We also investigate the effect of BD parameter. In addition, we study the free energy of BD black holes as well. The last section is devoted to closing remarks.

II. BLACK HOLES SOLUTIONS IN BDM GRAVITY

Regarding $(n+1)$-dimensional BDM theory, one finds related action as [10]

$$I_G = -\frac{1}{16\pi}\int_{\mathcal{M}} d^{n+1}x\sqrt{-g}\left(\Phi\mathcal{R} - \frac{\omega}{\Phi}(\nabla\Phi)^2 - V(\Phi) - F_{\mu\nu}F^{\mu\nu}\right), \tag{1}$$

where Φ and $V(\Phi)$ are, respectively, a scalar field and its self-interacting potential. Besides, the factor ω is the coupling constant, $\mathcal{R}$ is the scalar curvature, $F_{\mu\nu} = \partial_\mu A_\nu - \partial_\nu A_\mu$ is the electromagnetic tensor field and A_μ is the electromagnetic potential. Equations of motion can be obtained with the following explicit forms by varying the action (1) with respect to the gravitational field $g_{\mu\nu}$, the scalar field Φ and the gauge field A_μ [10]

$$\begin{aligned} G_{\mu\nu} &= \frac{\omega}{\Phi^2}\left(\nabla_\mu\Phi\nabla_\nu\Phi - \frac{1}{2}g_{\mu\nu}(\nabla\Phi)^2\right) - \frac{V(\Phi)}{2\Phi}g_{\mu\nu} + \frac{1}{\Phi}\left(\nabla_\mu\nabla_\nu\Phi - g_{\mu\nu}\nabla^2\Phi\right) \\ &\quad + \frac{2}{\Phi}\left(F_{\mu\lambda}F^{\lambda}_{\nu} - \frac{1}{4}F_{\rho\sigma}F^{\rho\sigma}g_{\mu\nu}\right), \end{aligned} \tag{2}$$

$$\nabla^2\Phi = -\frac{n-3}{2\left[(n-1)\omega+n\right]}F^2 + \frac{1}{2\left[(n-1)\omega+n\right)]}\left[(n-1)\Phi\frac{dV(\Phi)}{d\Phi} - (n+1)\,V(\Phi)\right], \tag{3}$$

$$\nabla_\mu F^{\mu\nu} = 0, \tag{4}$$

where $G_{\mu\nu}$ and ∇_μ are, respectively, the Einstein tensor and covariant derivative of manifold $\mathcal{M}$ with metric $g_{\mu\nu}$. Due to the appearance of inverse powers of the scalar field on the right hand side of (2), solving the field equations (2)-(4), directly, is a non-trivial task. This difficulty can be removed, by using a suitable conformal transformation [10]. Indeed, via the conformal transformation the BDM theory can be transformed into the Einstein-Maxwell theory with a minimally coupled scalar dilaton field. Suitable conformal transformation can be shown as [10]

$$\bar{g}_{\mu\nu} = \Phi^{2/(n-1)}g_{\mu\nu}, \tag{5}$$

$$\bar{\Phi} = \frac{n-3}{4\alpha}\ln\Phi, \tag{6}$$

where

$$\alpha = (n-3)/\sqrt{4(n-1)\omega+4n}. \tag{7}$$

It is worth mentioning that all functions and quantities in Jordan frame ($g_{\mu\nu}$, Φ and $F_{\mu\nu}$) can be transformed into Einstein frame ($\bar{g}_{\mu\nu}$, $\bar{\Phi}$ and $\bar{F}_{\mu\nu}$). Applying the mentioned conformal transformation on the BD action (1), one finds the action of dilaton gravity

$$\bar{I}_G = -\frac{1}{16\pi}\int_{\mathcal{M}} d^{n+1}x\sqrt{-\bar{g}}\left\{\bar{\mathcal{R}} - \frac{4}{n-1}(\bar{\nabla}\bar{\Phi})^2 - \bar{V}(\bar{\Phi}) - \exp\left(-\frac{4\alpha\bar{\Phi}}{(n-1)}\right)\bar{F}_{\mu\nu}\bar{F}^{\mu\nu}\right\}, \tag{8}$$

where $\bar{\nabla}$ and $\overline{\mathcal{R}}$ are, respectively, the covariant derivative and Ricci scalar corresponding to the metric $\bar{g}_{\mu\nu}$, and $\bar{V}(\bar{\Phi})$ is

$$\bar{V}(\bar{\Phi}) = \Phi^{-(n+1)/(n-1)}V(\Phi). \tag{9}$$

Regarding $(n+1)$-dimensional Einstein-Maxwell-dilaton action (8), α is an arbitrary constant that governs the strength of coupling between the dilaton and Maxwell fields. One can obtain the equations of motion by varying this action (8) with respect to $\bar{g}_{\mu\nu}$, $\bar{\Phi}$ and $\bar{F}_{\mu\nu}$

$$\bar{\mathcal{R}}_{\mu\nu} = \frac{4}{n-1}\left(\bar{\nabla}_\mu\bar{\Phi}\bar{\nabla}_\nu\bar{\Phi} + \frac{1}{4}\bar{V}\bar{g}_{\mu\nu}\right) + 2e^{-4\alpha\bar{\Phi}/(n-1)}\left(\bar{F}_{\mu\lambda}\bar{F}^{\lambda}_{\nu} - \frac{1}{2(n-1)}\bar{F}_{\rho\sigma}\bar{F}^{\rho\sigma}\bar{g}_{\mu\nu}\right), \tag{10}$$

$$\bar{\nabla}^2\bar{\Phi} = \frac{n-1}{8}\frac{\partial\bar{V}}{\partial\bar{\Phi}} - \frac{\alpha}{2}e^{-4\alpha\bar{\Phi}/(n-1)}\bar{F}_{\rho\sigma}\bar{F}^{\rho\sigma}, \tag{11}$$

$$\partial_\mu\left[\sqrt{-\bar{g}}e^{-4\alpha\bar{\Phi}/(n-1)}\bar{F}^{\mu\nu}\right] = 0. \tag{12}$$

Assuming the $\left(\bar{g}_{\mu\nu}, \bar{F}_{\mu\nu}, \bar{\Phi}\right)$ as solutions of Eqs. (10)-(12) with potential $\bar{V}\left(\bar{\Phi}\right)$ and comparing Eqs. (2)-(4) with Eqs. (10)-(12), the solutions of Eqs. (2)-(4) with potential $V(\Phi)$ can be written as

$$[g_{\mu\nu}, F_{\mu\nu}, \Phi] = \left[\exp\left(-\frac{8\alpha\bar{\Phi}}{(n-1)(n-3)}\right)\bar{g}_{\mu\nu}, \bar{F}_{\mu\nu}, \exp\left(\frac{4\alpha\bar{\Phi}}{n-3}\right)\right]. \tag{13}$$

As a consequence, we can solve Eqs. (10)-(12) with suitable potential, instead of solving Eqs. (2)-(4). Assuming an $(n+1)$-dimensional static and spherically symmetric metric

$$d\bar{s}^2 = -f(r)dt^2 + \frac{dr^2}{f(r)} + r^2R^2(r)d\Omega^2_{n-1}, \tag{14}$$

where $d\Omega^2_{n-1}$ is the metric of a unit $(n-1)$-sphere, and $f(r)$ and $R(r)$ are metric functions. By integrating the Maxwell equation (12), we can obtain the nonzero electric field $\bar{F}_{tr}$ as

$$\bar{F}_{tr} = \frac{q}{(rR)^{n-1}}\exp\left(\frac{4\alpha\bar{\Phi}}{n-1}\right), \tag{15}$$

where q is an integration constant related to electric charge. Now, we regard the following Liouville-type potential to solve the field equations

$$\bar{V}(\bar{\Phi}) = 2\Lambda\exp\left(\frac{4\alpha\bar{\Phi}}{n-1}\right) + \frac{(n-1)(n-2)\alpha^2}{c^2\left(\alpha^2-1\right)}e^{\frac{4\bar{\Phi}}{(n-1)\alpha}}. \tag{16}$$

Taking into account the metric (14) with Maxwell field (15) and potential (16), the consistent solutions of Eqs. (10) and (11) are [18]

$$\begin{aligned} f(r) &= -\frac{(n-2)\left(\alpha^2+1\right)^2c^{-2\gamma}r^{2\gamma}}{(\alpha^2+n-2)\left(\alpha^2-1\right)} + \frac{2\Lambda(\alpha^2+1)^2c^{2\gamma}}{(n-1)(\alpha^2-n)}r^{2(1-\gamma)} - \frac{m}{r^{(n-2)}}r^{(n-1)\gamma} \\ &\quad + \frac{2q^2(\alpha^2+1)^2c^{-2(n-2)\gamma}}{(n-1)(\alpha^2+n-2)r^{2(n-2)(1-\gamma)}}, \end{aligned} \tag{17}$$

$$R(r) = \exp(\frac{2\alpha\bar{\Phi}}{n-1}) = \left(\frac{c}{r}\right)^{\gamma}, \tag{18}$$

$$\bar{\Phi}(r) = \frac{(n-1)\alpha}{2(1+\alpha^2)}\ln(\frac{c}{r}), \tag{19}$$

where m is an integration constant which is related to the total mass, c is another arbitrary constant related to the scalar field and $\gamma = \alpha^2/(1+\alpha^2)$.

Now, using the conformal transformation, we are able to obtain the solutions of Eqs. (2)–(4). Considering the following spherically symmetric metric

$$ds^2 = -U(r)dt^2 + \frac{dr^2}{V(r)} + r^2 H^2(r) d\Omega_{n-1}^2, \tag{20}$$

with Eqs. (2)-(4), we find that the functions $U(r)$ and $V(r)$ are [18]

$$\begin{aligned} U(r) &= \frac{2\Lambda(\alpha^2+1)^2 c^{2\gamma(\frac{n-5}{n-3})}}{(n-1)(\alpha^2-n)} r^{2(1-\frac{\gamma(n-5)}{n-3})} - \frac{mc^{(\frac{-4\gamma}{n-3})}}{r^{(n-2)}} r^{\gamma(n-1+\frac{4}{n-3})} \\ &+ \frac{2q^2(\alpha^2+1)^2 c^{-2\gamma(n-2+\frac{2}{n-3})}}{(n-1)(\alpha^2+n-2) r^{2[(n-2)(1-\gamma)-\frac{2\gamma}{n-3}]}} - \frac{(n-2)\left(\alpha^2+1\right)^2}{(\alpha^2+n-2)\left(\alpha^2-1\right)} \left(\frac{c}{r}\right)^{-2\gamma\left(\frac{n-1}{n-3}\right)}, \end{aligned} \tag{21}$$

$$\begin{aligned} V(r) &= \frac{2\Lambda(\alpha^2+1)^2 c^{2\gamma(\frac{n-1}{n-3})}}{(n-1)(\alpha^2-n)} r^{2(1-\frac{\gamma(n-1)}{n-3})} - \frac{mc^{(\frac{4\gamma}{n-3})}}{r^{(n-2)}} r^{\gamma(n-1-\frac{4}{n-3})} \\ &+ \frac{2q^2(\alpha^2+1)^2 c^{-2\gamma(n-2-\frac{2}{n-3})}}{(n-1)(\alpha^2+n-2) r^{2[(n-2)(1-\gamma)+\frac{2\gamma}{n-3}]}} - \frac{(n-2)\left(\alpha^2+1\right)^2}{(\alpha^2+n-2)\left(\alpha^2-1\right)} \left(\frac{c}{r}\right)^{-2\gamma\left(\frac{n-5}{n-3}\right)}, \end{aligned} \tag{22}$$

where we used the conformal transformation of Eq. (16) with the following explicit form

$$V(\Phi) = 2\Lambda\Phi^2 + \frac{(n-1)(n-2)\alpha^2}{c^2\left(\alpha^2-1\right)} \Phi^{[(n+1)(1+\alpha^2)-4]/[(n-1)\alpha^2]}. \tag{23}$$

In addition, one can use the conformal transformation to obtain consistent electromagnetic field as

$$F_{tr} = \frac{qc^{(3-n)\gamma}}{r^{(n-3)(1-\gamma)+2}}. \tag{24}$$

As one can see, the electromagnetic field becomes zero as $r \longrightarrow \infty$. It is evident that as $\omega \longrightarrow \infty$, the obtained solutions are just the charged solutions of Einstein gravity (RN AdS black hole).

Using the Euclidian action, the finite mass and the entropy of the black hole can be obtained [10]

$$M = \frac{c^{(n-1)\gamma}}{16\pi} \left(\frac{n-1}{1+\alpha^2}\right) m, \tag{25}$$

$$S = \frac{c^{(n-1)\gamma}}{4} r_+^{(n-1)(1-\gamma)}. \tag{26}$$

By considering the flux of electric field at infinity, one can find the total charge of this configuration as

$$Q = \frac{q}{4\pi}. \tag{27}$$

Calculations show that the Hawking temperature of a BD black hole on the outer horizon r_+ is

$$T = \frac{\kappa}{2\pi} = \frac{1}{4\pi}\sqrt{\frac{V}{U}} \left(\frac{dU}{dr}\right)\Big|_{r=r_+}, \tag{28}$$

where κ is the surface gravity. After some simplifications, we obtain [18]

$$\begin{aligned} T &= -\frac{2(1+\alpha^2)}{4\pi(n-1)} \left(\Lambda c^{2\gamma} r_+^{1-2\gamma} + \frac{q^2 c^{-2(n-2)\gamma}}{{r_+}^{\gamma}} {r_+}^{(2n-3)(\gamma-1)}\right) \\ &+ \frac{\left[\gamma(n-3)-n+2\right](1-n)(n-2)}{2r_+\left(\alpha^2+n-2\right)\left(\alpha^2-1\right)} \left(\frac{c}{r_+}\right)^{-2\gamma}. \end{aligned} \tag{29}$$

III. STABILITY, PHASE TRANSITION AND GEOMETRICAL THERMODYNAMICS

In this section, first, we study stability and phase transition of the solutions in the context of the heat capacity. Next, we consider the geometrical approach for studying phase transition. We investigate the effect of BD parameter and compare the results of both approaches.

There are several approaches for studying the stability of black holes. One of these approaches is related to studying the perturbed black holes and see if and how they acquire stable state and will be in equilibrium. This approach is known as dynamical stability of black holes. In this paper, we are not interested in dynamical stability of black holes. We focus our studies on the thermal stability of charged black hole solutions in the context of BD theory through canonical ensemble. To do so, we calculate the heat capacity and study its behavior.

Black holes should have a positive heat capacity in order to be thermally stable. In other words, the positivity of the heat capacity guarantees the local thermal stability of the black holes. One can use the following relation for the heat capacity

$$C_Q = T\left(\frac{\partial^2 M}{\partial S^2}\right)_Q^{-1} = T\left(\frac{\partial S}{\partial T}\right)_Q = T\left(\frac{\partial S}{\partial r_+}\right)_Q\left(\frac{\partial T}{\partial r_+}\right)_Q^{-1}. \tag{30}$$

On the other hand, it is possible to employ the heat capacity for studying the phase transitions of black holes. In the context of black holes, it is argued that root of the heat capacity ($C_Q = T = 0$) is representing a border line between physical ($T > 0$) and non-physical ($T < 0$) black holes. We call it physical limitation point. The system in case of this physical limitation point has a change in sign of the heat capacity. In addition, it is believed that the divergencies of the heat capacity are representing phase transitions of black holes. These phase transitions known as second order phase transition [19]. Therefore, the phase transition and limitation points of the black holes in the context of the heat capacity are calculated with the following relations

$$\begin{cases} T = \left(\frac{\partial M}{\partial S}\right)_Q = 0, & \textit{physical limitation point} \\ \left(\frac{\partial^2 M}{\partial S^2}\right)_Q = 0, & \textit{second order phase transition} \end{cases}. \tag{31}$$

Regarding Eq. (31) and in order to find physical limitation point, one should solve the following equation for the entropy

$$\begin{aligned}\left(\frac{\partial M}{\partial S}\right)_Q &= 7\frac{\pi^2\Lambda\left(n-9-4\omega\right)A_1 c^{(n+1)j_1}}{4} + \frac{\left(n-2\right)\pi^2\left[\left(n-1\right)\omega+n\right]A_2 c^{(n-3)j_1}}{2} \\ &+\frac{\left(n-9-4\omega\right)Q^2}{c^{(n-3)j_1}A_2} = 0,\end{aligned} \tag{32}$$

while as for the second order phase transition points (divergence points of the heat capacity), we obtain the following relation

$$\begin{aligned}\left(\frac{\partial T}{\partial S}\right)_Q &= \frac{\pi^2\Lambda\left(n-9-4\omega\right)A_1 c^{(n+1)j_1}}{32} - \frac{\left(n-2\right)\pi^2\left[\left(n-1\right)\omega+n\right]A_2 c^{(n-3)j_1}}{16} \\ &+\frac{\left[\left(n-12\right)\omega+9\left(n-1\right)\right]Q^2}{8A_2 c^{(n-3)j_1}} = 0,\end{aligned} \tag{33}$$

where

$$A_1 = \left(c^{-\frac{(n-3)^2}{(4n-4)\omega+4n}}\left(4S\right)^{\frac{n^2+(4\omega-2)n+9-4\omega}{4[(\omega+1)n-\omega](n-1)}}\right)^{j_2},$$

$$A_2 = \left(c^{-\frac{(n-3)^2}{(4n-4)\omega+4n}}\left(4S\right)^{\frac{n^2+(4\omega-2)n+9-4\omega}{4[(\omega+1)n-\omega](n-1)}}\right)^{j_3},$$

$$j_1 = \zeta\left(n-3\right)^2,$$

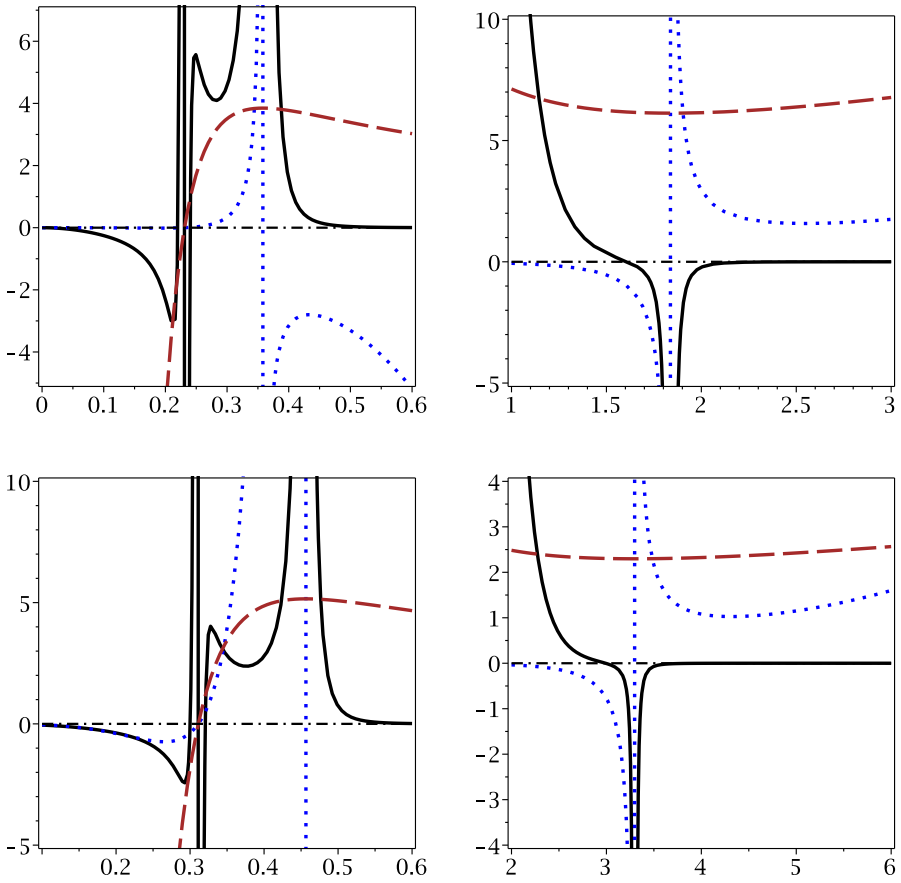

FIG. 1: For different scales: $\mathcal{R}$ (continuous line), C_Q (dotted line) and T (dashed line) versus r_+ for $\Lambda = -1$, $\omega = 1$, $c = 1$ and $q = 0.1$. (up diagrams: $d = 5$ & down diagrams: $d = 6$)

$$j_2 = \zeta \left[4n\omega \left(n-1\right) + 3n \left(n+1\right) + 3n - 9\right],$$

$$j_3 = \zeta \left(n-1\right) \left[\left(4n-8\right)\omega + 5n - 9\right],$$

$$\zeta = \left[\left(n-1\right)^2 + 4 \left(n-1\right)\omega + 8\right]^{-1}.$$

It is worthwhile to mention that for the case of physical limitation point, numerical evaluation shows that there is only one root for this case which will be seen by plotted graphs for the heat capacity. In the case of phase transition point, interestingly, numerical evaluation shows that two cases might happen: in one of these cases, there is no real root for Eq. (33), hence there is no phase transition for the black holes. Whereas in the other case, due to the structure of Eq. (33), there will be two roots for this equation which indicate the existence of two divergence points, and therefore, could be interpreted as phase transition for these black holes. This will be seen in plotted graphs (Figs. 1-5) in more details.

Another approach for studying the phase transition of black holes is through geometrical thermodynamics. There are several metrics that one can employ in order to build geometrical phase space by thermodynamical quantities. The well known ones are Ruppeiner, Weinhold and Quevedo. It was previously argued that these metrics may not provide us a completely flawless mechanism for studying geometrical thermodynamics of specific types of black holes [25]. In this paper, we will show that the method of geometrical thermodynamics reported in [26] is not suitable in the presence of scalar field. Recently, a new metric (HPEM metric) was proposed in order to solve the problems that other metrics may confront with [25].

According to Ref. [27], it is possible to derive, in principle, an infinite number of Legendre invariant metrics. In addition, it was shown that one of the simplest ways for obtaining the Legendre invariant metrics is to apply a

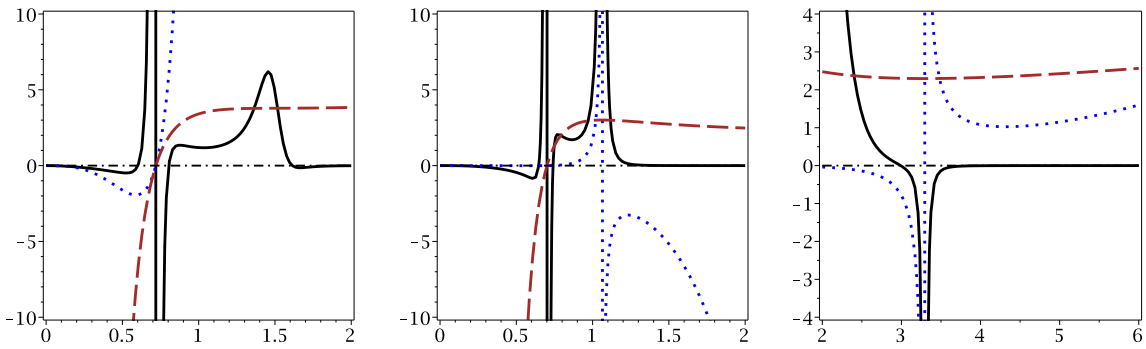

FIG. 2: For different scales: $\mathcal{R}$ (continuous line), C_Q (dotted line) and T (dashed line) versus r_+ for $\Lambda=-1$, $\omega=1$, $c=1$ and $q=1$. (left diagram: $d=5$ & middle and right diagrams: $d=6$)

conformal transformation. Comparing HPEM metric with Quevedo's one, we find that they are the same up to a conformal factor. In addition, despite Weinhold and Ruppeiner, both HPEM and Quevedo metrics enjoy the same $(-+++...)$ signature. Regarding the same signature with difference in conformal factor, it is expected that HPEM enjoys Legendre invariancy with different Legendre multiplier.

On the other hand, we should mention an unavoidable comment related to Legendre invariancy. Although it was thought that the Legendre invariancy guarantees unique description of thermodynamical metrics, it was shown that such invariancy alone is not sufficient for the mentioned guarantee in terms of thermodynamical curvatures [28]. However, it was proven that in addition to Legendre invariancy, we need to demand curvature invariancy in various representations. Therefore, both Legendre and curvature invariancies should be checked. In addition, there are two issues with a fundamental relation between them; (I) agreement of thermodynamical curvature results with usual thermodynamical approaches (such as the heat capacity); (II) curvature invariancy in addition to the Legendre invariancy. It is important to probe the fundamentality of cases (I) and (II) for discovering that regarding which case may lead to satisfy another one. Although first case has been investigated for special cases [28], the second one has been remained unanalyzed yet. One may address them in an independent work in the future.

The Weinhold, Ruppeiner and Quevedo thermodynamical metrics are given by

$$ds_W^2=Mg_{ab}^W dX^a dX^b, \tag{34}$$

$$ds_R^2=-MTg_{ab}^W dX^a dX^b, \tag{35}$$

$$ds_Q^2=\left(SM_S+QM_Q\right)\left(-M_{SS}dS^2+M_{QQ}dQ^2\right), \tag{36}$$

where $g_{ab}^W=\partial^2 M\left(X^c\right)/\partial X^a\partial X^b$ and also $X^a\equiv X^a\left(S,N^i\right)$, in which N^i denotes other extensive variables of the system. The HPEM metric, with 2 extensive parameters (entropy and electric charge), is

$$ds_{HPEM}^2=\frac{SM_S}{M_{QQ}^3}\left(-M_{SS}dS^2+M_{QQ}dQ^2\right), \tag{37}$$

where $M_X=\left(\frac{\partial M}{\partial X}\right)$ and $M_{XX}=\left(\frac{\partial^2 M}{\partial X^2}\right)$. Calculations show that the numerator and denominator of HPEM method for this type of thermodynamical system are given as [25]

$$\begin{aligned} num(\mathcal{R}_{HPEM}) \;=\; & 6S^2M_S^2M_{QQ}M_{SS}^2M_{QQQQ}-6SM_S^2M_{QQ}^2M_{SS}M_{SSQQ}+2SM_{SQQ}^2M_S^2M_{QQ}M_{SS} \\ & +2\left[SM_SM_{SSS}-\frac{1}{2}M_{SS}\left(SM_{SS}-M_S\right)\right]SM_{QQ}^2M_SM_{SQQ}-9S^2M_{QQQ}^2M_S^2M_{SS}^2 \\ & +4\left[\frac{1}{4}M_{SQ}M_{SS}+M_SM_{SSQ}\right]S^2M_{QQ}M_SM_{QQQ}+\left[S^2M_S^2M_{SSQ}-S^2M_{SQ}M_{SS}M_SM_{SSQ}\right. \\ & \left. SM_{QQ}M_S\left(SM_{SS}-M_S\right)M_{SS}-2\left(S^2M_{SS}^3+M_S^2M_{SS}\right)M_{QQ}+2S^2M_{SQ}^2M_{SS}^2\right]M_{QQ}^2, \end{aligned} \tag{38}$$

and

$$denom(\mathcal{R}_{HPEM})=S^3M_S^3M_{SS}^2. \tag{39}$$

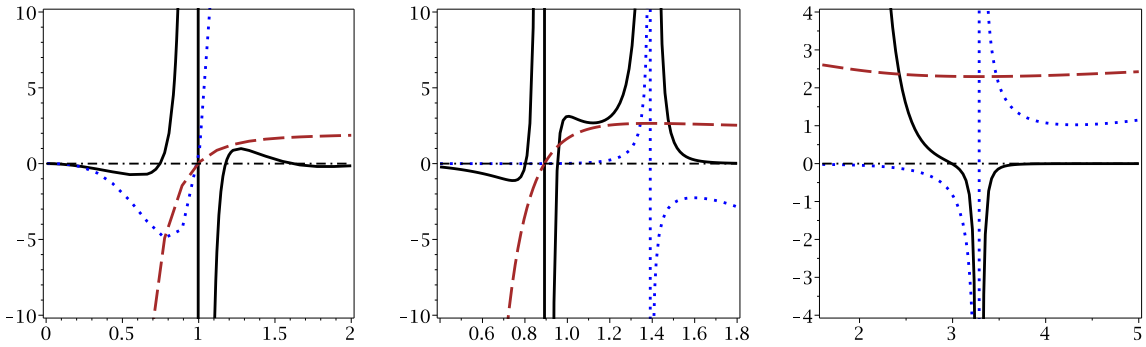

FIG. 3: For different scales: $\mathcal{R}$ (continuous line), C_Q (dotted line) and T (dashed line) versus r_+ for $\Lambda = -1$, $\omega = 1$, $c = 1$ and $q = 2$. (left diagram: $d = 5$ & middle and right diagrams: $d = 6$)

It is obvious that in general, the roots of the numerator and denominator of this Ricci scalar are not coinciding. Meaning that the case, where the divergency of Ricci scalar could be cancelled by its root, does not take place. The denominator of Ricci scalar of HPEM metric contains numerator and denominator of the heat capacity. In other words, divergence points of the Ricci scalar of HPEM metric coincide with both roots and phase transition points of the heat capacity. Therefore, all the phase transition and limitation points are included in the divergencies of Ricci scalar of this metric.

In what follows, we study the stability and phase transition of the charged BD black holes in the context of canonical ensemble by calculating heat capacity. Then, we study geometrical thermodynamics of these black holes by using the HPEM thermodynamical metric. Before conducting the research in the context of HPEM method, we will show that Weinhold, Ruppeiner and Quevedo metrics fail to provide effective results.

First of all, one should take this fact into consideration that the sign of temperature is putting a restriction of system being physical or non-physical. In other words, the negativity of temperature denotes a non-physical system which in our case is black hole. It is evident that, there is a critical horizon radius, say r_c, in which for $r_+ < r_c$ the temperature of the system is negative. Therefore, in this region solutions are non-physical. Since for $r_+ > r_c$ system has positive temperature, the horizon radius of physical black holes are placed in this region.

In case of 5–dimensional black holes, for sufficiently small values of electric charge (Fig. 1 top), BD coupling constant (Fig. 4 top), these black holes have three characteristic points. One is related to the root of heat capacity and the others are related to its divergencies (r_{Div1} and r_{Div2} in which $r_{Div1} < r_{Div2}$). It is clear that the root of heat capacity and r_c are the same and for the case $r_+ < r_c$ the heat capacity is negative but due to negativity of temperature, the system is not physical. On the other hand, for the region $r_c < r_+ < r_{Div1}$, heat capacity is positive definite. Therefore, in this region, the system is in a stable state. As for the $r_{Div1} < r_+ < r_{Div2}$ the heat capacity has a negative value which is denoted as instability of the black holes. In other words, in case of $r_+ = r_{Div1}$ system may go under phase transition from large and unstable black hole to a smaller and stable one. In case of $r_+ = r_{Div2}$ system will have another phase transition and its stability will change from unstable to stable one. In other words, for $r_+ > r_{Div2}$ the heat capacity has a positive value and the black hole is stable. It is notable that for sufficiently large values of q (Figs. 2 and 3 left), ω (Fig. 5 left), divergencies of the heat capacity vanish and the black hole is thermally stable for $r_+ > r_c$, without any phase transition.

In case of 6–dimensional charged BD black holes, we find the following results. It is clear that in case of 6–dimensional, using considered values in case of 5–dimensional solutions, in all cases one root and two divergence points for heat capacity are observed. In these cases, heat capacity and phase transitions have similar behavior as what was observed in 5–dimensions charged BD black holes. r_{Div1} is an increasing function of electric charge (Figs. 2 and 3 middle) while r_{Div2} is a decreasing function of BD coupling constant (Figs. 2 and 5 right). We should note that the effects of variation of q is so small on second divergence point (Figs. 2 and 3 right).

Next, by employing the metrics that were defined, Eqs. (34)-(37), we construct a thermodynamical spacetime with mass as thermodynamical potential. Using Eqs. (25)–(27) one can write total mass of the black holes as a function of extensive parameters. By employing Eqs. (34)-(37) the spacetime will be constructed. Next, we calculate the curvature scalar of the mentioned thermodynamical metrics. Analytical calculations of the curvature scalar is too large and, therefore, we leave out the analytical result for reasons of economy.

Studying Fig. 6 shows that using Weinhold and Ruppeiner leads to a mismatch between divergency of the Ricci scalar of these two metrics and divergency of the heat capacity. In other words, the phase transitions of the Ruppeiner and Weinhold metrics do not coincide with phase transitions of the canonical ensemble, hence, heat capacity. Next,

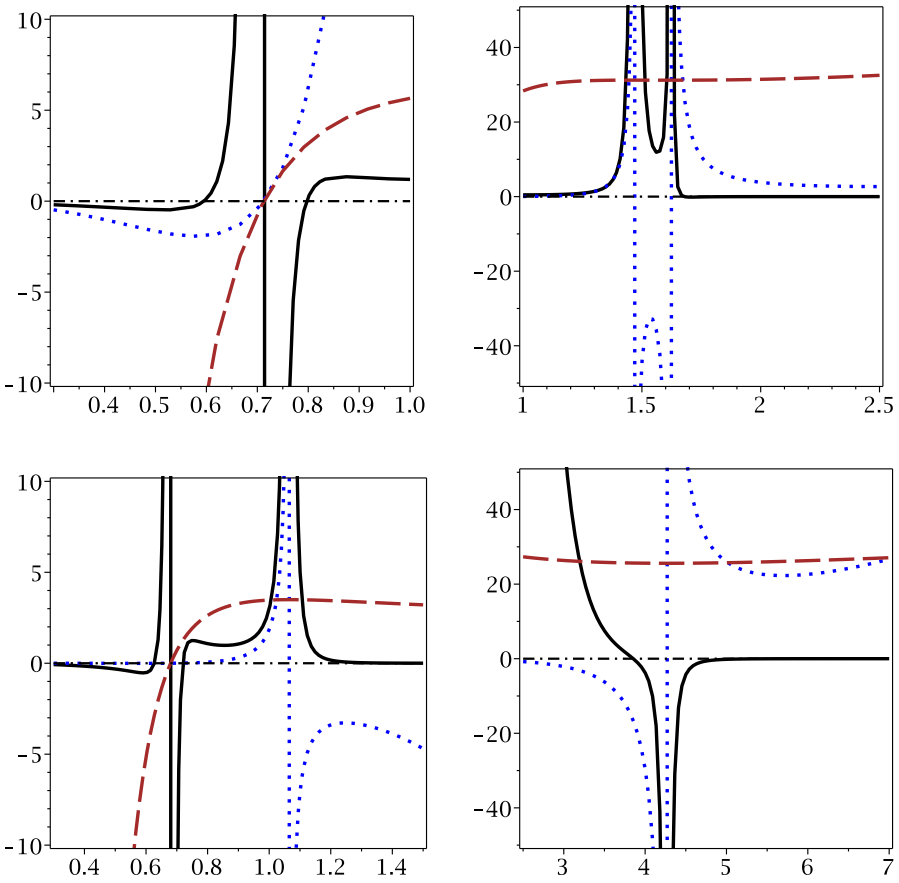

FIG. 4: For different scales: $\mathcal{R}$ (continuous line), C_Q (dotted line) and T (dashed line) versus r_+ for $\Lambda = -1$, $q = 1$, $c = 1$ and $\omega = 0.1$. (up diagrams: $d = 5$ & down diagrams: $d = 6$)

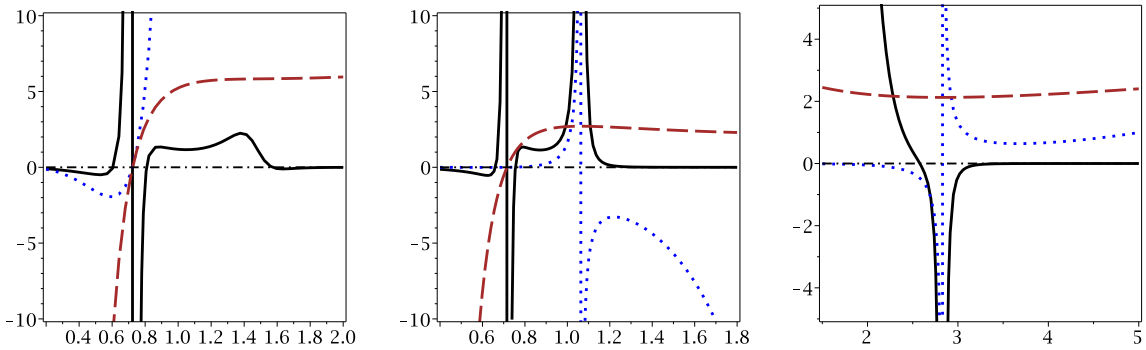

FIG. 5: For different scales: $\mathcal{R}$ (continuous line), C_Q (dotted line) and T (dashed line) versus r_+ for $\Lambda = -1$, $q = 1$, $c = 1$ and $\omega = 3$. (left diagram: $d = 5$ & middle and right diagrams: $d = 6$)

we present the behavior of obtained results for HPEM method in plotted graphs (Figs. 1-5). These figures show that divergencies of thermodynamical Ricci scalar coincide with root and divergence points of the heat capacity. As for Quevedo metric, we will follow another approach to show that it fails to produce suitable results. It is a matter of calculation to show that using Quevedo metric (36), one can find following denominator for its Ricci scalar

$$denom(\mathcal{R}_Q) = (SM_S + QM_Q)^3 M_{SS}^2 M_{QQ}^2. \tag{40}$$

Here, three terms contribute to divergencies of the Ricci scalar of Quevedo metric. M_{SS} ensures that phase

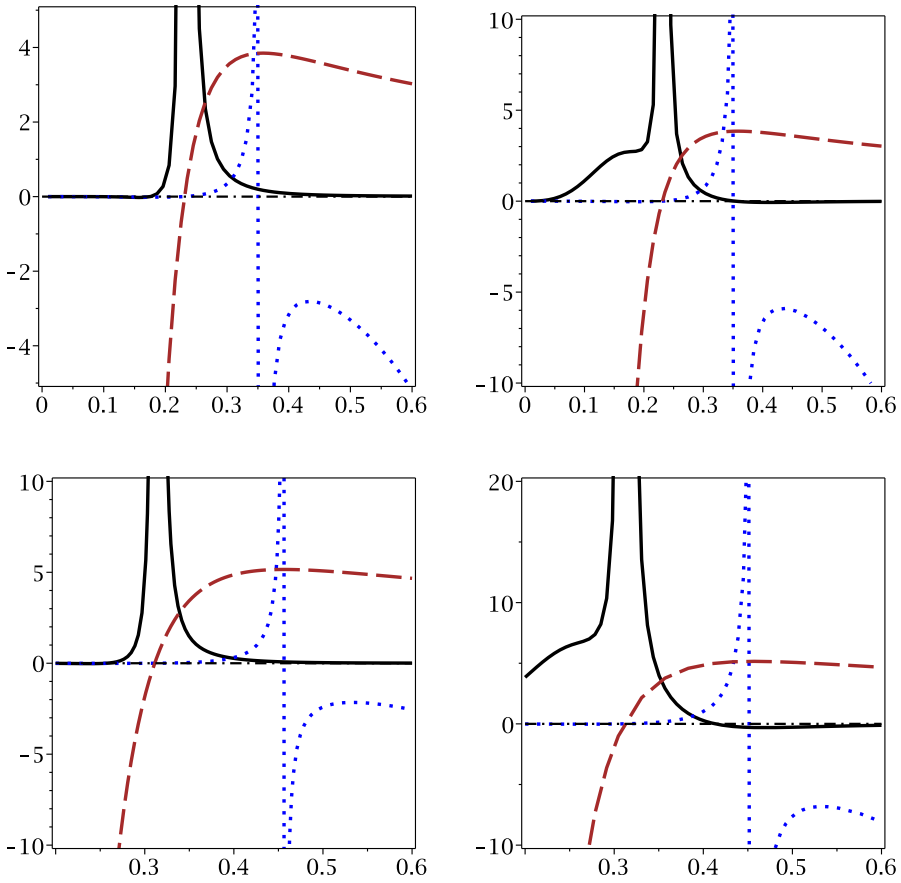

FIG. 6: Left panel: Weinhold, right panel: Ruppeiner; $\mathcal{R}$ (continuous line), C_Q (dotted line) and T (dashed line) versus r_+ for $\Lambda = -1$, $\omega = 1$, $c = 1$ and $q = 0.1$. (up diagrams: $d = 5$ & down diagrams: $d = 6$)

transitions of the heat capacity and some of the divergencies of the Ricci scalar of this metric coincide, where the other two terms will result into extra divergencies that are not coincidence with any phase transition. In other words, the results of using this metric are not consistent with the results of heat capacity. Therefore, if one uses this metric independent of heat capacity, due to being plugged with extra divergencies, it is not possible to make acceptable statements regarding the physical properties of the system. For further clarification, we give an example. For $d = 5$ and $\Lambda = \omega = c = 1$, one can find the following relation for the Ricci scalar of Quevedo metric

$$R = \frac{-104799744\pi^2\, r_+^{\frac{228}{29}}}{841\,\Gamma_1^2\,\Gamma_2^3}\Big\{11981115\, r_+^{\frac{390}{29}} - 8575308\, r_+^{\frac{336}{29}} - 83387808\, r_+^{\frac{282}{29}} + 116784640\, r_+^{\frac{228}{29}} - 5880114\, r_+^{\frac{222}{29}} + 33781860\, r_+^{\frac{168}{29}} + 343570752\, r_+^{\frac{114}{29}} - 123023853\, r_+^{\frac{54}{29}} - 133929936\Big\}, \tag{41}$$

where Γ_1 term

$$\Gamma_1 = 9\, r_+^{\frac{168}{29}} + 28\, r_+^{\frac{114}{29}} - 47, \tag{42}$$

in the denominator, ensures that all the divergencies of the heat capacity are coincided with some of the divergencies of the Ricci scalar, whereas, Γ_2 term

$$\Gamma_2 = 171\, r_+^{\frac{168}{29}} - 532\, r_+^{\frac{114}{29}} - 333, \tag{43}$$

provides extra divergencies, which are not matched with any phase transition point. It is worthwhile to mention that the root of numerator does not cancel extra divergencies of the Ricci scalar. Therefore, this simple example shows that Quevedo metric is plugged with extra divergencies which are not consistent with phase transition points.

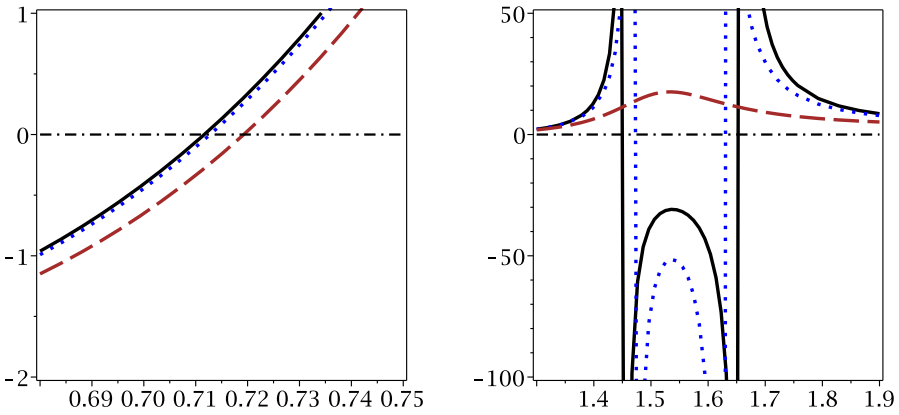

FIG. 7: For different scales: C_Q versus r_+ for $\Lambda = -1$, $c = 1$, $d = 5$, $q = 1$ and $\omega = 0.01$ (continues line), $\omega = 0.1$ (dotted line) and $\omega = 1$ (dashed line).

Therefore, HPEM metric provides a successful mechanism for studying the places of root and phase transition points of these black holes in context of canonical ensemble. It is worthwhile to mention that the behavior of the thermodynamical Ricci scalar is different around root and divergence points of the heat capacity. In other words, in case of divergency of Ricci scalar coinciding with the root of heat capacity, the behavior of the diagrams differs from the case in which divergency of the Ricci scalar coincides with divergencies of heat capacity. Therefore, considering HPEM method, we find that the root and phase transitions are distinguishable from one another. In order to recognize physical limitation point (r_c) from phase transition points, one can extract the following information from the figures. In case of root of heat capacity ($S = S_0$), hence, physical limitation point, there is a change in sign of Ricci scalar from $+\infty$ to $-\infty$. Whereas for the case of the divergence points of the heat capacity, hence, second order phase transitions, the sign of the Ricci scalar stays fixed. Therefore, this change/unchange in sign is a characteristic that enables one to distinguish root of heat capacity from phase transition points. We summarize the mentioned information in table I.

	C_Q	$\mathcal{R}$
$S = S_0$	$\lim_{S\to S_0} C_Q = 0$	$\lim_{S\to S_0^-} \mathcal{R} = +\infty$ $\lim_{S\to S_0^+} \mathcal{R} = -\infty$
$S = S_{1c}$	$\lim_{S\to S_{1c}^-} C_Q = +\infty$ $\lim_{S\to S_{1c}^+} C_Q = -\infty$	$\lim_{S\to S_\infty^-} \mathcal{R} = +\infty$ $\lim_{S\to S_\infty^+} \mathcal{R} = +\infty$
$S = S_{2c} > S_{1c}$	$\lim_{S\to S_{2c}^-} C_Q = -\infty$ $\lim_{S\to S_{2c}^+} C_Q = +\infty$	$\lim_{S\to S_\infty^-} \mathcal{R} = -\infty$ $\lim_{S\to S_\infty^+} \mathcal{R} = -\infty$

Table I: comparison of root with phase transition points

Regarding C_Q versus entropy, numerical calculations and also figures show that the heat capacity has a real positive root (S_0) for all values of parameters (q, ω, Λ, c). For the case of divergence points of heat capacity, there are two cases. In first case and for special choices of parameters, heat capacity does not diverge, while for second case, one can set free parameters in such a way that C_Q has two real positive divergence points (S_{1c} and S_{2c}).

In order to emphasize the effects of the Brans-Dicke gravity, we have plotted Figs. 7 and 8 for variation of ω. It is evident that the variation of the Brans-Dicke parameter modifies the number of the divergencies and roots and their corresponding places. These modifications lead to changes in stability conditions (regions of the stability) as well as phase transitions of the black holes. This shows that in presence of modified gravity (Brans-Dicke gravity), the thermodynamical structure of the black holes will be modified and acquires different structure comparing to the absence of Brans-Dicke gravity.

According to the pioneering work of Davies [19], regarding phase transitions in black holes, the divergencies of the heat capacity are second order phase transition. In his works, he showed that these divergencies of the heat capacity have characteristics of the second order phase transition. In addition, the studies that are conducted in extended phase space proved that divergencies of the heat capacity, and second order phase transition in phase diagrams, coincide with each other [29]. In other words, second order phase transition points that are observed in Gibbs free

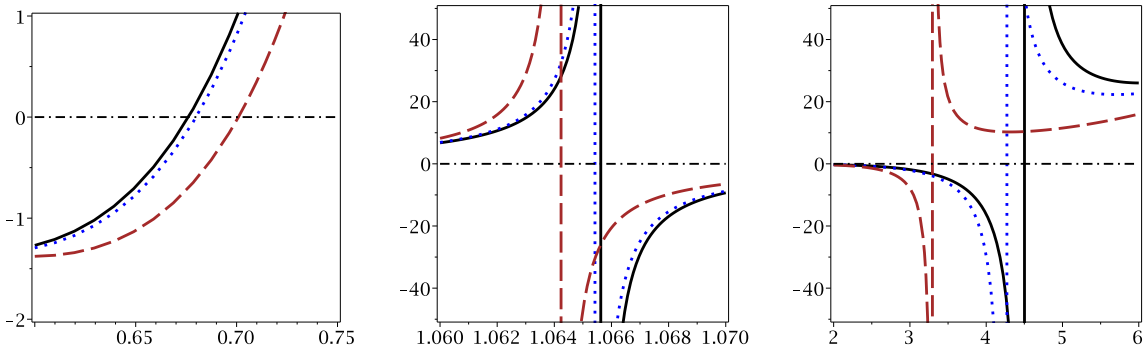

FIG. 8: For different scales: C_Q versus r_+ for $\Lambda = -1$, $c = 1$, $d = 6$, $q = 1$ and $\omega = 0.01$ (continues line), $\omega = 0.1$ (dotted line) and $\omega = 1$ (dashed line).

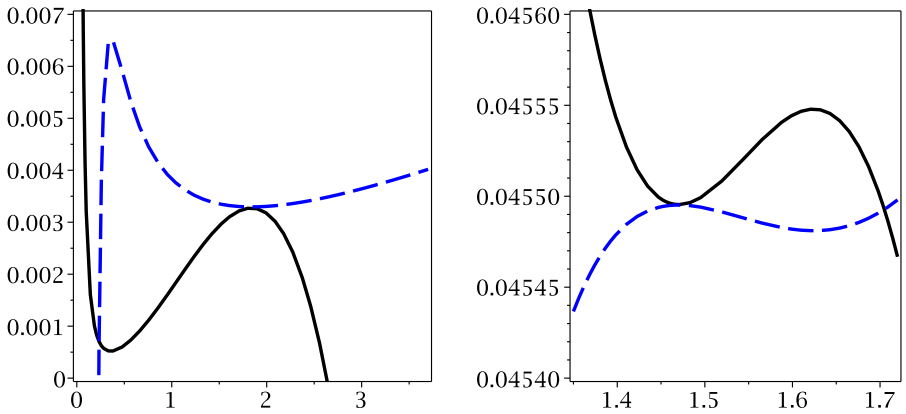

FIG. 9: For different scales: F (continuous line) and T (dashed line) versus r_+ for $\Lambda = -1$, $c = 1$ and $d = 5$. (left diagram: $\omega = 1$ and $q = 0.1$ & right diagram: $q = 1$ and $\omega = 0.1$)

energy versus temperature, pressure versus horizon radius and temperature versus horizon radius, are matched with divergencies of the heat capacity. Therefore, the divergencies of the heat capacity are second order phase transitions. For more clarifications, we will study corresponding free energy versus horizon radius as well.

The free energy for these black holes is given by

$$F = M - TS,$$

in which by using Eqs. (25), (26) and (29), one can find free energy as

$$F = \frac{\zeta\left[n\left(n-2\right)+4\omega\left(n-1\right)\right]}{4\pi j_3}\left\{\frac{q^2\left[n\left(\omega+\frac{9}{8}\right)-\frac{3}{2}\omega-\frac{9}{8}\right]}{\left[\omega\left(n-1\right)+n\right]c^{j_1}r^{j_3}}+\frac{\left(n-2\right)c^{j_1}r^{j_3}}{4}\right.$$
$$\left.-\frac{\Lambda\left(n-4\omega-9\right)\left[n\left(\omega+\frac{5}{4}\right)-2\omega-\frac{9}{4}\right]c^{(n+1)j_1}r^{\zeta(n-1)[3(3n+1)+4n\omega]}}{2\left[\omega\left(n-1\right)+n\right]\left[n\left(3+4\omega\right)+9\right]}\right\}. \tag{44}$$

Now, by employing this relation and specific choices of different parameters in plotted diagrams, we plot following figures (9-11).

Thermodynamically speaking, in free energy diagrams, the second order phase transition takes place when the free energy acquires an extremum. Here, we see for these specific choices of the different parameters, free energy has two extrema. These extrema are located exactly where temperature has extrema as well. The existence of extrema in the temperature is observed as divergencies in the heat capacity. Therefore, the extrema of free energy, where second order phase transition takes place, coincide with divergencies of the heat capacity. This leads to the conclusion that divergencies that are observed in the heat capacity are where black holes go under second order phase transition.

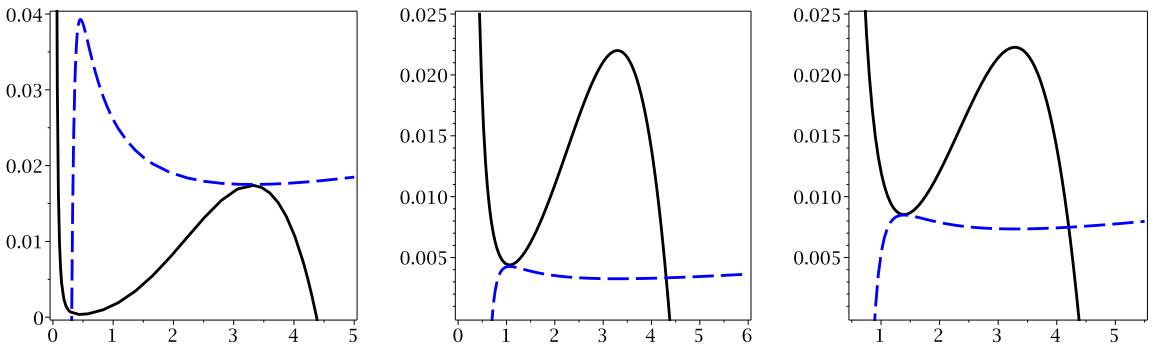

FIG. 10: For different scales: F (continuous line) and T (dashed line) versus r_+ for $\Lambda = -1$, $c = 1$, $d = 6$ and $\omega = 1$. (left diagram: $q = 0.1$ & middle diagram: $q = 1$ & right diagram: $q = 2$)

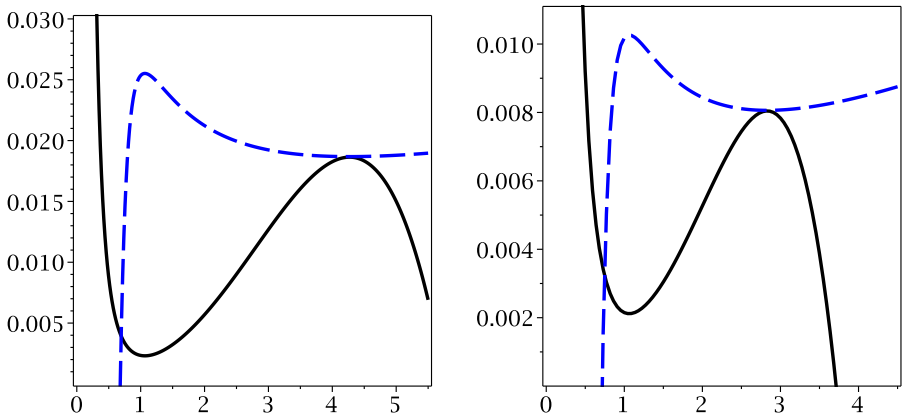

FIG. 11: For different scales: F (continuous line) and T (dashed line) versus r_+ for $\Lambda = -1$, $c = 1$, $d = 6$ and $q = 1$. (left diagram: $\omega = 0.1$ & right diagram: $\omega = 3$)

Furthermore, we calculate critical horizon radius and temperature by $\left(\frac{\partial T}{\partial r_+}\right)$ and present the results in table II. In order to compare the results of heat capacity with those of $T - r_+$ diagram and HPEM approach for calculating the critical horizon radius, we combine all results in table II. It is evident from obtained values for critical horizon radius and their corresponding critical temperature that they coincide with extrema in free energy and divergencies of the heat capacity as well. This shows that phase transition points which are second order ones are consistent for free energy, temperature and heat capacity as well. Therefore, divergencies of the heat capacity in fact are places in which second order phase transitions take place.

d	q	ω	$T-r_+$ diagram: $T_c\rightarrow$	$T-r_+$ diagram: $r_c\rightarrow$	$F-r_+$ diagram: $r_c\rightarrow$	C_Q-r_+ diagram: $r_c\rightarrow$
5	0.1	1	0.38486	0.35794	0.35794	0.35794
			0.19380	1.83804	1.83804	1.83804
5	1	0.1	0.19709	1.47014	1.47014	1.47014
			0.19703	1.62412	1.62412	1.62412
6	0.1	1	0.51557	0.45643	0.45643	0.45643
			0.22972	3.29845	3.29845	3.29845
6	1	1	0.30070	1.06423	1.06423	1.06423
			0.22969	3.29541	3.29541	3.29541
6	2	1	0.26534	1.39027	1.39027	1.39027
			0.22963	3.28597	3.28597	3.28597
6	1	0.1	0.34958	1.06542	1.06542	1.06542
			0.25592	4.27029	4.27029	4.27029
6	1	3	0.27082	1.06333	1.06333	1.06333
			0.21270	2.83018	2.83018	2.83018

Table II: Critical horizon radius and temperature for $\Lambda=-1$ and $c=1$.

IV. CLOSING REMARKS

In this paper, we have studied the thermal stability and phase transitions of charged BD black holes in context of canonical ensemble by calculating the heat capacity. We showed that there is a lower bound for the horizon radius of physical charged BD black holes. This restriction was originated from the sign of the temperature of these black holes. We found that the regions of the physical and non–physical black holes were functions of electric charge and BD coupling constant.

Regarding the phase transition of the black holes, we found that black holes in the context of BD enjoy the existence of second order phase transition. In other words, the heat capacity of these black holes diverged in two points and it had a real valued positive root. It was pointed out that the existence of the divergence points and their places were functions of q and ω. It is worthwhile to mention that the effect of variation of electric charge on larger divergence point was relatively so small. This small effect indicates that the existence of the larger divergence point is due to contribution of the BD gravity. It was also seen that dimensions changed the existence of the divergence points of the heat capacity and also the places of the root and divergencies of it. It is notable to mention that these black holes have three characteristic points which are related to positive temperature and thermal (in)stability of these black holes.

In the context of thermal stability, it was pointed out that there are four regions with different conditions. These regions are specified by the root and two divergencies of the heat capacity. In case of root of the heat capacity, there was a limitation point between non-physical black holes and physical ones. Between two divergencies, it was an unstable state and after the larger divergency it acquired stable state. In other words, in smaller divergency black hole may go under phase transition from unstable state with larger horizon radius to smaller stable black hole, whereas, in case of larger divergency system went under another phase transition and stabilized with larger horizon radius.

Finally, we used the geometrical thermodynamics for studying phase transitions of the system. It was shown that the divergencies of the curvature scalar of the HPEM metric exactly coincide with both physical limitation point and phase transitions of the heat capacity. In other words, divergencies of the heat capacity and its root are matched with divergencies of the Ricci scalar. It was also shown unlike RN-AdS black holes [26] (in the absence of dilaton field), employing Weinhold, Ruppeiner and Quevedo metrics failed to provide effective results for BD black hole solutions. It is notable that the behavior of the Ricci scalar around its divergence points for root and phase transitions was different. It means that, there were characteristic behaviors that enable one to recognize divergence point of Ricci scalar related to root of the heat capacity from divergence points of $\mathcal{R}$ related to divergencies of C_Q. Therefore, one is able to point out that physical limitation point and phase transitions took place in the divergencies of thermodynamical Ricci scalar of the HPEM metric with different distinctive behaviors.

In addition, the free energy of these black holes has been investigated as well. It was shown that free energy enjoys extrema in its diagrams versus horizon radius. These extrema were located exactly where temperature acquires extrema and heat capacity diverges. It was pointed out that divergencies that are observed in heat capacity are places where black holes go under second order phase transition.

Acknowledgements

We would like to thank the referees for their constructive comments. We also thank the Shiraz University Research Council. This work has been supported financially by the Research Institute for Astronomy and Astrophysics of Maragha, Iran.

---

[1] B. P. Abbott et al. Phys. Rev. Lett. **116**, 061102 (2016).
[2] C. Corda, JCAP **04**, 009 (2007);
S. Capozziello and C. Corda, Int. J. Mod. Phys. D **15**, 1119 (2006);
C. Corda, Astropart. Phys. **28**, 247 (2007);
C. Corda, Astropart. Phys. **30**, 209 (2008);
S. Capozziello, C. Corda and M. F. De Laurentis, Phys. Lett. B, **669**, 255 (2008);
C. Corda, Int. J. Mod. Phys. D **18**, 2275 (2009).
[3] S. Perlmutter et al., Astrophys. J. **517**, 565 (1999);
S. Perlmutter, M. S. Turner and M. White, Phys. Rev. Lett. **83**, 670 (1999);
A. G. Riess et al., Astrophys. J. **607**, 665 (2004).
[4] S. Weinberg: Gravitation and Cosmology (Wiley, 1972);
P. A. M. Dirac: Proc. R. Soc. Lond. A **165**, 199 (1938).
[5] T. Clifton, P. G. Ferreira, A. Padilla and C. Skordis, Phys. Rep. **513**, 1 (2012).
[6] K. Bamba and S. D. Odintsov, JCAP **04**, 024 (2008);
G. Cognola, E. Elizalde, S. Nojiri, S. D. Odintsov, L. Sebastiani and S. Zerbini, Phys. Rev. D **77**, 046009 (2008);
C. Corda, Europhys. Lett. **86**, 20004 (2009);
T. P. Sotiriou and V. Faraoni, Rev. Mod. Phys. **82**, 451 (2010);
S. Capozziello, F. Darabi and D. Vernieri, Mod. Phys Lett A **25**, 3279 (2010);
S. H. Hendi, B. Eslam Panah and S. M. Mousavi, Gen. Relativ. Gravit. **44**, 835 (2012);
S. G. Ghosh and S. D. Maharaj, Phys. Rev. D **85**, 124064 (2012);
Y. S. Myung, Phys. Rev. D **88**, 104017 (2013);
S. H. Hendi, B. Eslam Panah and R. Saffari, Int. J. Mod. Phys. D **23**, 1450088 (2014).
[7] C. Brans and R. Dicke, Phys. Rev. **124**, 925 (1961).
[8] M. A. Scheel, S. L. Shapiro and S. A. Teukolsky, Phys. Rev. D **51**, 4208 (1995);
M. A. Scheel, S. L. Shapiro and S. A. Teukolsky, Phys. Rev. D **51**, 4236 (1995);
G. Kang, Phys. Rev. D **54**, 7483 (1996);
H. P. de Oliveira and E. S. Cheb-Terrab, Class. Quantum Gravit. **13**, 425 (1996).
[9] S. W. Hawking, Commun. Math. Phys. **25**, 167 (1972).
[10] R. G. Cai and Y. S. Myung, Phys. Rev. D **56**, 3466 (1997);
M. H. Dehghani, J. Pakravan and S. H. Hendi, Phys. Rev. D **74**, 104014 (2006);
S. H. Hendi, J. Math. Phys. **49**, 082501 (2008);
S. H. Hendi and R. Katebi, Eur. Phys. J. C **72**, 2235 (2012).
[11] S. W. Hawking, Comm. Math. Phys. **43**, 199 (1975).
[12] M. Henneaux and C. Teitelboim, Phys. Lett. B **143**, 415 (1984);
M. Henneaux and C. Teitelboim, Phys. Lett. B **222**, 195 (1989).
[13] C. Teitelboim, Phys. Lett. B **158**, 293 (1985).
[14] Y. Sekiwa, Phys. Rev. D **73**, 084009 (2006);
E. A. Larranaga Rubio, [arXiv:0711.0012];
[15] J. D. Brown and C. Teitelboim, Phys. Lett. B **195**, 177 (1987);
J. D. Brown and C. Teitelboim, Nucl. Phys. B **297**, 787 (1988).
[16] B. Dolan, Class. Quantum Gravit. **28**, 125020 (2011);
M. Cvetic, S. Nojiri and S. D. Odintstov, Nucl. Phys. B **628**, 295 (2002).
[17] J. Creighton and R. B. Mann, Phys. Rev. D **52**, 4569 (1995);
M. M. Caldarelli, G. Cognola and D. Klemm, Class. Quantum Gravit. **17**, 399 (2000);
D. Kastor, S. Ray and J. Traschen, Class. Quantum Gravit. **26**, 195011 (2009);
B. P. Dolan, Phys. Rev. D **84**, 127503 (2011);
B. P. Dolan, Class. Quantum Gravit. **28**, 235017 (2011);
B. P. Dolan, [arXiv:1209.1272];
M. Cvetic, G. W. Gibbons, D. Kubiznak and C. N. Pope, Phys. Rev. D **84**, 024037 (2010);
D. Kubiznak and R. B. Mann, JHEP **033**, 1207 (2012);
S. Gunasekaran, D. Kubiznak and R. B. Mann, JHEP **11**, 110 (2012);;
S. H. Hendi and M. H. Vahidinia, Phys. Rev. D **88**, 084045 (2013);
S. H. Hendi, S. Panahiyan and R. Mamasani, Gen. Relativ. Gravit. **47**, 91 (2015);
R. G. Cai, L. M. Cao, L. Li, and R. Q. Yang, JHEP **09**, 005 (2013);

S. H. Hendi, S. Panahiyan and B. Eslam Panah, Prog. Theor. Eexp. Phys. **2015**, 103E01 (2015).
[18] S. H. Hendi and Z. Armanfard, Gen. Relativ. Gravit. **47**, 125 (2015).
[19] P. Davies, Proc. R. Soc. A **353**, 499 (1977).
[20] F. Weinhold, J. Chem. Phys. **63**, 2479 (1075);
F. Weinhold, J. Chem. Phys. **63**, 2484 (1975).
[21] G. Ruppeiner, Phys. Rev. A **20**, 1608 (1979);
G. Ruppeiner, Rev. Mod. Phys. **67**, 605 (1995).
[22] P. Salamon, J. D. Nulton and E. Ihrig, J. Chem. Phys. **80**, 436 (1984).
[23] H. Quevedo, Gen. Relativ. Gravit. **40**, 971 (2008);
H. Quevedo, A. Sanchez, S. Taj and A. Vazquez, Gen. Relativ. Gravit. **43**, 1153 (2011);
A. Bravetti, D. Momeni, R. Myrzakulov and H. Quevedo, Gen. Relativ. Gravit. **45**, 1603 (2013);
H. Quevedo and A. Sanchez, JHEP **09**, 034 (2008).
[24] R. G. Cai and J. H. Cho, Phys. Rev. D **60**, 067502 (1999);
J. E. Aman, I. Bengtsson and N. Pidokrajt, Gen. Relativ. Gravit. **35**, 1733 (2003);
J. E. Aman and N. Pidokrajt, Phys. Rev. D **73**, 024017 (2006);
G. Arciniega and A. Sanchez, [arXiv:1404.6319];
S. H. Hendi and R. Naderi, Phys. Rev. D **91**, 024007 (2015).
[25] S. H. Hendi, S. Panahiyan, B. Eslam Panah and M. Momennia, Eur. Phys. J. C **75**, 507 (2015);
S. H. Hendi, S. Panahiyan and B. Eslam Panah, Adv. High Energy Phys. **2015**, 743086 (2015);
S. H. Hendi, A. Sheykhi, S. Panahiyan and B. Eslam Panah, Phys. Rev. D **92**, 064028 (2015);
S. H. Hendi, B. Eslam Panah and S. Panahiyan, JHEP **05**, 029 (2016).
[26] C. Niu and Y. Tian and X. N. Wu, Phys. Rev. D **85**, 024017 (2012).
[27] H. Quevedo, Gen. Relativ. Gravit. **40**, 971 (2008);
[28] A. Bravetti, C. S. L. Monsalvo, F. Nettel and H. Quevedo, J. Math. Phys. **54**, 033513 (2013).
[29] S. H. Hendi, B. Eslam Panah and S. Panahiyan, JHEP **11**, 157 (2015);
M. S. Ma and R. Zhao, Phys. Lett. B **751**, 278 (2015);
S. H. Hendi, S. Panahiyan and B. Eslam Panah, Int. J. Mod. Phys. D **25**, 1650010 (2016);
S. H. Hendi, S. Panahiyan and B. Eslam Panah, JHEP **01**, 129 (2016);
J. X. Mo, G. Q. Li and Y. C. Wu, JCAP **04**, 045 (2016).